2nd URSI AT-RASC, Gran Canaria, 28 May – 1 June 2018

A domain decomposition method to simulate the response of biological cell systems exposed to radio frequency

Sebastian Böhmelt, Nils Kielian, Michael Dudzinski, Marco Rozgic and Marcus Stiemer*
Helmut Schmidt University, University of the Federal Armed Forces Hamburg

Abstract

A combination of a domain decomposition algorithm and a finite element method for the efficient three dimensional simulation of electro-quasistatic multi-scale problems is presented and applied to the simulation of the dielectric properties of biological cell suspensions. In this scheme, cells and membranes are discretized by meshes fitted to their geometrical scales. The simulation can be carried out for all considered cells in parallel. The data exchange between the particular meshes relies on Robin boundary conditions assuring the conservation of fluxes according to Maxwell's equations. Efficient algorithms are provided for data exchange between the meshes. From simulation results, biologically relevant quantities, such as the transmembrane potential, are computed.

1 Introduction

Suspensions of biological cells exhibit a typical dispersion behavior when exposed to electromagnetic fields [9]: A high value of its relative permittivity for low frequencies falls down to the value of the suspension medium (typically water) within the frequency range between 10 kHz and 10 MHz. This behavior is a consequence of the periodic charging and discharging of the capacitors composed by the electrically badly conducting cell membrane and the relatively well conducting inner and outer regions of the cell. The formation of a capacitive field over the cell membrane is associated with a relaxation constant, whose magnitude in comparison to the period of the triggering field determines the effective capacitance of the cell, and hence, the susceptibility of the cell suspension for polarization.
An interest in a deeper insight in a cell's polarization in an exterior electromagnetic field emerges from several points: to understand the impact of radio frequencies on biological cells, to compute the electrical properties of cell solutions, or to solve the inverse problem in order to identify cell types from spectroscopical properties of the solution. Cell properties can, e.g., be concluded from a cell's trajectory in an inhomogeneous electric field, see [13].
Analytical homogenization techniques for suspensions of spherical particles and of spherical shells have been introduced by Debye [6] and applied by, e.g., Schwan and Foster in a biological context [8, 17]. An electro-quasi-static (EQS) approximation to Maxwell's equations is relevant in this case [5], since the wavelengths occurring in the respective frequency domain are much larger than the dimensions of a cell, which amount to approximately 1 µm for many types of cells, and since electrical induction may be neglected. First attempts at the numerical simulation of the polarization of single cells have been presented by Asami et al. [1] based on difference methods and later on finite element (FE) simulations [4], allowing for a better representation of complex geometries. Further applications of these methods are presented, e.g., in [2, 3].
The simulation of cell systems which are exposed to electromagnetic fields faces two crucial problems: first, the simulation of an individual cell defines a multi scale problem, since the membrane is 2-3 orders of magnitude smaller than the cell itself. Second, a homogenization method is required to derive the electric properties of the whole system from the study of a small number of individual cells.
In this article, a method is presented, which reaches both objectives in an efficient way by a combination of a domain decomposition algorithm as presented by Lions [14, 15, 16] and an FE-simulation of the EQS-system. In this scheme, cells and membranes are discretized by meshes fitted to their geometrical scales. The simulation can be carried out for all considered cells in parallel. The data exchange between the particular meshes relies on Robin boundary conditions assuring the conservation of fluxes according to Maxwell's equations. In contrast to [5], a thee dimensional setting is considered here, and more efficient mesh coupling algorithms are employed. Both the time harmonic and the transient case have been implemented, although the presentation will focus on the time harmonic case. From simulation results, biologically relevant quantities, such as the transmembrane potential, are computed. The algorithm is implemented in a fast object oriented library [7].

2 Domain decomposition and EQS-model

In the following, ∇ represents the nabla operator, and hence, $\nabla\times$ denotes the curl-, $\nabla\cdot$ the divergence-, and ∇ the gradient-operator. If biological cells are exposed to radio frequencies in the range between 10 kHz and 10 MHz, wave phenomena may be neglected, since possible waves possess wave lengths on a much larger scale than the size of the cells. While capacitive fields are significant, electric induc-

tion can be neglected, i.e., the approximation $\nabla \times \vec{E} = \vec{0}$ is valid, and an electric scalar potential

$$\vec{E} = -\nabla\varphi \tag{1}$$

exists. Applying $\nabla\cdot$ on the Ampère-Maxwell law

$$\nabla \times \vec{H} = \vec{J} + \frac{\partial \vec{D}}{\partial t} \tag{2}$$

in this situation and profiting from the material relations

$$\begin{aligned} \vec{J} &= \kappa\vec{E} \\ \vec{D} &= \varepsilon_r\varepsilon_0\vec{E} \end{aligned} \tag{3}$$

with electric field constant ε_0 for linear isotropic materials with conductivity κ and relative permittivity ε_r leads together with the potential relation (1) to

$$\nabla\cdot\left(\kappa\nabla\varphi + \varepsilon\nabla\frac{\partial\varphi}{\partial t}\right) = 0\,. \tag{4}$$

Now the whole domain Ω is considered partitioned in a collection of subdomains Ω_i, $i = 1,\ldots,N$, with mutual interfaces $\Gamma_{ik} = \overline{\Omega}_i \cap \overline{\Omega}_k$, which may be empty. In the following, a quantity indexed with i denotes the restriction of that field to the subdomain Ω_i. On nonempty interfaces Γ_{ik}, the following continuity relations hold (for simplicity, we just demonstrate the case $i = 2$ and $k = 1$ without loss of generality) due to the continuity of the potential, the conservation of electric fluxes and the continuity equation:

$$\varphi_2 - \varphi_1 = 0\,, \tag{5}$$

$$\vec{n}\cdot\left(\vec{D}_2 - \vec{D}_1\right) = \sigma_{21}\,, \tag{6}$$

$$\vec{n}\cdot\left(\vec{J}_2 - \vec{J}_1\right) = -\frac{\partial\sigma_{21}}{\partial t} \tag{7}$$

for the electric flux density $\vec{D} = -\varepsilon_r\varepsilon_0\nabla\varphi$ and the current density $\vec{J} = -\kappa\nabla\varphi$ on the interface. Here σ_{21} denotes a temporally and spatially varying surface charge density on the interface between the two neighboring domains.
In time harmonic setting the potential can be represented by

$$\varphi(\vec{r},t) = \mathrm{Re}\left(\underline{\varphi}(\vec{r})\exp(\mathrm{j}\omega t)\right) \tag{8}$$

where $\underline{\varphi}$ fullfills the model equation

$$\nabla\cdot\left(\underline{\kappa}\nabla\underline{\varphi}\right) = 0 \tag{9}$$

of the EQS-system, where $\underline{\kappa} = \kappa + \mathrm{j}\omega\varepsilon_r\varepsilon_0$ denotes the complex conductivity for angular frequency ω. Equation 5 yields the Dirichlet-boundary-condition

$$\underline{\varphi}_1\Big|_{\Gamma_{21}} = \underline{\varphi}_2\Big|_{\Gamma_{21}}\,. \tag{10}$$

while a comparison of (7) and the time derivative of (6) leads to the Neumann-boundary condition

$$\underline{\kappa}_1\frac{\partial\underline{\varphi}_1}{\partial n}\bigg|_{\Gamma_{21}} = \underline{\kappa}_2\frac{\partial\underline{\varphi}_2}{\partial n}\bigg|_{\Gamma_{21}}\,, \tag{11}$$

holding at the same time with the derivative $\frac{\partial}{\partial n}$ in the direction of the normal vector pointing from Ω_1 to Ω_2. Following [14, 15, 16] the conditions 10 and 11 are combined to a Robin type boundary condition, i.e., a linear combination of both, to enable a parallel computation on each subdomain of the decomposed domain:

$$\underline{\varphi}_1 + \lambda\underline{\kappa}_1\frac{\partial\underline{\varphi}_1}{\partial n}\bigg|_{\Gamma_{21}} = \underline{\varphi}_2 + \lambda\underline{\kappa}_2\frac{\partial\underline{\varphi}_2}{\partial n}\bigg|_{\Gamma_{21}}\,. \tag{12}$$

The choice of the positive parameter λ influences the speed of the convergence of the iteration [5]. Starting from any estimate for the Robin boundary data on each non empty interface Γ_{ik}, the system (8) can be solved in any Ω_i, yielding a set of new Robin boundary conditions on all interfaces. This process will then be iterated until the condition

$$\int_{\Gamma_{ik}}\left|\underline{\varphi}_k^\ell - \underline{\varphi}_i^\ell\right|^2\,\mathrm{d}s \le \delta \tag{13}$$

holds on each interface Γ_{ik} for a chosen threshold $\delta > 0$. Here, the upper index denotes the iteration number ℓ, and integration is carried out with respect to arc length. To avoid the evaluation of the numerically badly conditioned gradient in (12), the right hand sides in these Robin boundary conditions can be computed iteratively via two sequences of functions $\underline{g}_i^\ell$, $i = 1,2$, $\ell \in \mathbb{N}$ [10]. Hence, the boundary conditions take the form

$$\underline{\varphi}_i^\ell + \lambda\underline{\kappa}_i\nabla\underline{\varphi}_i^\ell\cdot\vec{n} = \underline{g}_i^\ell\,, \tag{14}$$

with $i = 1,2$. The functions $\underline{g}_i^\ell$ can conveniently be computed during itration via the update formulae

$$\begin{aligned} \underline{g}_1^{\ell+1} &= 2\underline{\varphi}_2^\ell - \underline{g}_2^\ell\,, \\ \underline{g}_2^{\ell+1} &= 2\underline{\varphi}_1^\ell - \underline{g}_1^\ell\,. \end{aligned} \tag{15}$$

3 Discretization and data exchange

To solve the FE problems occurring in each iteration step, an efficient implementation of the FE method is employed [7]. This leads to linear systems of equations whose right hand sides depend on data of the neighboring domains from the preceding time step. Hence, they can all be computed in parallel. As the computation time for FE procedures usually grows superlinear with increasing problem size, the iteration scheme does not only help to bridge different scales, but also leads to a reduction of computing time. To obtain the boundary data in each step, the solution computed on an interface in one domain must be evaluated at particular points to provide the associated degrees of freedom of the FE discretization in the neighboring domain. As long as any degree of freedom on one domain is one to one associated with one of the neighboring domain, this task is simple. However, for meshes on different scales it is not efficient to enforce that each degree of freedom is shared by the other mesh. Hence, interpolation techniques have to be applied. However, such methods lead to poor results,

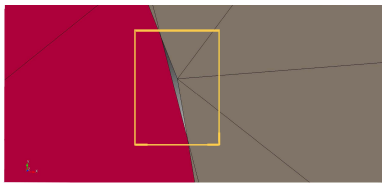

Figure 1. No associated point can be found for data transfer between the meshes [13].

if values for points have to be determined that are located outside the domain covered by the other mesh (see Figure 1). To avoid this problem, an auxiliary toroidal domain (in three dimensions) is patched over the interface such that the method originally formulated for non-overlapping domains becomes a scheme for overlapping domains as depicted in Figure 2: in the discretization of the original non-overlapping formulation of the interface problem (top) holes can in general not be avoided (middle): By introducing an auxiliary domain, whose boundary components are contained in exactly one of the two neighboring domains, the data transfer can be achieved by fast point location (bottom). The physical interface is now an interior surface of the auxiliary domain, where each vertex of one mesh on the interface corresponds to a geometrically identical vertex of the other mesh. For an efficient retrieval of corresponding points in the overlapping case an efficient point location algorithm has been implemented [12].

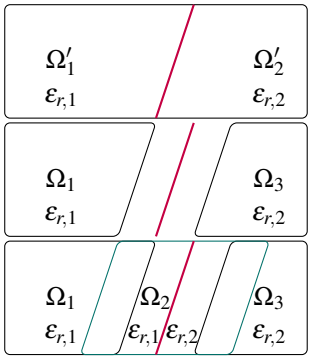

Figure 2. Original problem (top), discretization with hole (middle), and patched version (bottom) [13].

4 Some results on cell suspensions

Various versions of the model described above have been implemented and validated, and parameter studies have been carried out (e.g., [5, 11, 12, 13]). Figure 3 shows, e.g., the mesh of a CAD-model of a small cube of water containing an ellipsoidal cell. In Figure 4, the dispersion of the permittivity computed for such a system is displayed, where K denotes the ratio between the varied length of the two equally long smaller semi axes and the unique longer semi axis, which is held at constant size and aligned with those faces of the cube which serve as electrodes. The shape is varied from a sphere $K = 1$ to that of a rod $K = 8$. As

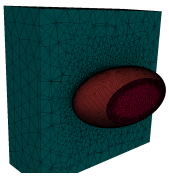

Figure 3. Meshed CAD-model of a cell in suspension [13].

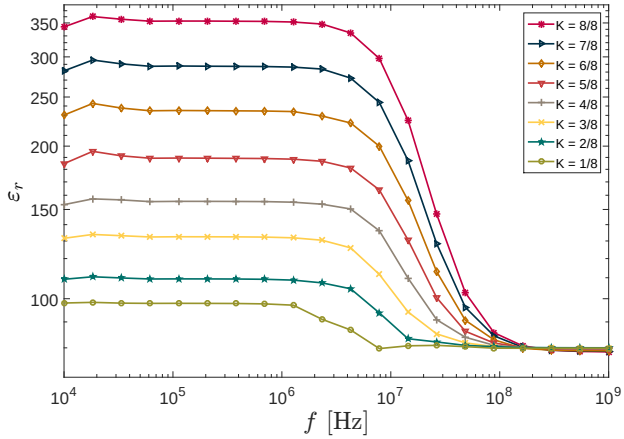

Figure 4. Dispersion curve for ellipsoidal cells with different aspect radii K [13].

expected, the sphere shows the highest capability for polarization, witch decreases with increasing deviation from the sphere. The different dispersion curves for different cell shapes correspond to a different polarization, and, hence to a different assumed dipole moment of the cell. Since an inhomogeneous electrical field yields a non-zero resulting force on a dipole, a separation of different cells (or other particles) based on different dispersion behavior becomes possible [13]. Further extended parameter studies includ-

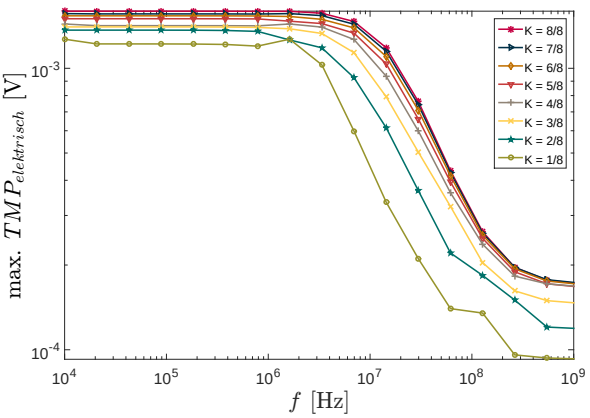

Figure 5. Change of the transmembrane potential (TMP) due to the external field for different aspect radii K.

ing different cell shapes and orientations have been carried out in [11]. With the help of the numerically determined

electric potential φ, the influence of the external field on a cell's transmembrane potential can, e.g., be determined. In Figure 5, the magnitude of the additional contribution is depicted for the cell models considered in Figure 4. The transmembrane potential takes a predominant role for a cell's nutrition and ion balance.

5 Conclusions and outlook

The presented domain decomposition algorithm has proven to lead to accurate results of electrical properties of cell systems. Its capability of parallel treatment makes it an efficient method to solve large EQS-systems. Hence, the electric properties of large systems of biological cells can be numerically studied, which offers a wide range of applications. A method for the numerical homogenization of biological multi-cell systems such as cell suspensions is, e.g., currently implemented. In this scheme, the interior of each cell and each cell membrane in a representative volume element as well as the surrounding medium are individually meshed. After application of the scheme described in this article, the mean permittivity of the cell suspension is computed as, e.g., shown in [5]. Further, the presented numerical method can be used to develop methods for the separation of particles, which are first polarized by an external field and then differently accelerated in an inhomogeneous electric field due to different dipole moments. A numerical method for this has already been presented in [13]. Another subsequent step is to study the electric properties of cell systems that arise when the polarization of substructures of cells are considered. This should lead to a further dispersion at higher frequencies that has not been examined yet. By also augmenting the simulation by resonating molecules, a realistic electromagnetic cell model should be reached step by step and used in biotechnological engineering and for the prediction of possible hazards.

References

[1] K. Asami, "Characterization of biological cells by dielectric spectroscopy," *J. Non-Cryst. Solids*, **305**, 2002, pp. 268–277.

[2] K. Asami, "Dielectric dispersion in biological cells of complex geometry simulated by the three-dimensional finite difference method," *J. Phys. D: Appl. Phys.*, **39**, 2006, pp. 492–499.

[3] K. Asami, "Effectiveness of Thin-Layer and Effective Medium Approximations in Numerical Simulation of Dielectric Spectra of Biological Cell Suspensions," *J. P. N. J. Appl. Phys.*, **49**, 2010, pp. 492–499.

[4] K. Asami, "Dielectric properties of microvillous cells simulated by the three-dimensional finite-element method," *Bioelectrochemistry*, **81**, 2011, pp. 28–33.

[5] S. Böhmelt, F. Scharf, M. Dudzinski, M. Rozgic, L. O. Fichte and M. Stiemer, "Finite element simulation of the frequency-dependent polarization of biological cells," *IEEE Int. Symp. EMC*, 2015, pp. 535-540.

[6] P. Debye, "Der Rotationszustand von Molekülen in Flüssigkeiten," *Physik. Zeits.*, **36**, 1935, p. 100.

[7] M. Dudzinski, M. Rozgic and M. Stiemer, "oFEM: An object oriented finite element package for MATLAB," *Applied Mathematics and Computation*, 2017, accepted.

[8] K. R. Foster, H. P. Schwan, "Dielectric properties of tissues and biological materials: A critical review," *Critical reviews in biomedical engineering*, **17**, 1989.

[9] M. Hofmann, "Integrierte Impedanzspektroskopie aerober Zellkulturen in biotechnologischen Hochdurchsatzscreenings," Ph.D. thesis, RWTH-Aachen, 2009.

[10] L. S. Huo and W. Guo, "Generalizations and accelerations of Lions' nonoverlapping domain decomposition method for linear elliptic PDE," *SIAM journal on numerical analysis*, **41(6)**, 2003, pp. 2056–2080.

[11] N. Kielian: "3D FEM Simulation of Biological Cells in Electromagnetic Fields: A Parameter Study," Bachelorthesis, Helmut Schmidt University, University of the Federal Armed Forces Hamburg, 2016.

[12] N. Kielian: "Point-Location and Interpolation for the Evaluation of Mesh-Functions in Domain-Decomposition Methods," Student Project, Helmut Schmidt University, University of the Federal Armed Forces Hamburg, 2017.

[13] N. Kielian: "Characterisation of Biological Cells by Electrical Fields: A Finite-Element-Based Approach," Masterthesis, Helmut Schmidt University, University of the Federal Armed Forces Hamburg, 2017.

[14] P. Lions, "On the Schwarz Alterrnating Method. I," *First Int. Symp. on Domain Decomposition Methods for Partial Differential Equations*, **1**, 1988, pp. 1–42.

[15] P. Lions, "On the Schwarz alternating method II," *Domain Decomposition Methods*, SIAM, Philapalphia, 1989.

[16] P. Lions, "On the Schwarz Alternating Method III: A Variant for Nonoverlapping Subdomains," *Third Int. Symp. on Domain Decomposition Methods for Partial Differential Equations*, **3**, 1990, pp. 202–231.

[17] H. P. Schwan, K. R. Foster, "RF-Field Interactions with Biological Systems: Electrical Properties and Biophysical Mechanisms," *Proc. IEEE*, **68**, 1980, pp. 104–113.